

## Totally Light Controlled Thyristor-Optically Triggerable and Optically Quenchable Static Induction Photo-Thyristor

Jun-ichi Nishizawa, Takashige Tamamushi<sup>†</sup>, and Ken-ichi Nonaka

Research Institute of Electrical Communication, Tohoku University, Sendai 980, Japan

<sup>†</sup>Semiconductor Research Institute, Kawauchi, Sendai 980, Japan

Optically Triggerable and optically quenchable Static Induction Photo-Thyristor (SIP Thy) is described in this paper concentrating on the optical direct/indirect Triggering and optical quenching mechanisms. Using only two LEDs driven by CMOS logic IC, 300V-2A is directly triggered and quenched in a turn-on time of 6.2 $\mu$ sec and a turn-off time of 15 $\mu$ sec, and 540V-1A is indirectly switched in a turn-on time of 545nsec and a turn-off time of 7.15 $\mu$ sec, until now.

### §1. Introduction

The device structure and the measured results of the fabricated devices of Static Induction Thyristor (SI Thyristor) were reported by J. Nishizawa et al. in 1972<sup>1)</sup>. The main operational principle of the SI Thyristor is the control of the potential barrier height by the static induction effect to modulate the forward current of the p-n diode.

SI Thyristor has many excellent features such as low forward voltage drop<sup>2)</sup>, high speed switching<sup>3)</sup>, high blocking gain<sup>2)</sup>, high breakdown voltage, high di/dt and high dv/dt capability<sup>4)</sup>, the high gate to cathode breakdown voltage, and being difficult to cause thermal breakdown at time of overcurrent break<sup>5)</sup>, compared to the conventional pnpn thyristor and gate-turn-off thyristor (GTO).

On the other hand, the idea of optical triggering of the SI Thyristor was proposed in 1975<sup>6)</sup> by analogy of the conventional Light Activated Thyristor. However, as is well-known, conventional Light Activated Thyristors have a weak point of its lengthy turn-off time during the commutative turn-off process. And also, to our knowledge, there is no report about optically-triggered and optically/electrically-quenched GTO. The experimental results of optical quenching (turn-off) of the conventional pnpn thyristor is reported in reference 8), where the high power p-i-n photodiode is antiparallely connected between anode and cathode of the conventional pnpn thyristor. However, it requires very high power light sources for the irradiation on the quenching p-i-n photodiode to turn-off the main thyristor commutatively. The concept of optical quenching of the SI Thyristor, which was proposed in 1979<sup>7)</sup>, is defined by the following optically-gate-turn-off operation that, if the light sensitive element, such as photoconductor, pin photodiode, Schottky diode, bipolar phototransistor, photothyristor etc., is connected or integrated to the gate terminal of the SI Thyristor, it can be optically quenched by the optical irradiation on the light sensitive element, because the amount of stored holes at the gate electrode of the SI Thyristor during the turn-on state can be discharged through

the light sensitive element.

In 1983, optical direct triggering and optical quenching operation of the SI Thyristor was experimentally confirmed by the authors<sup>9,10)</sup> using only two LEDs for direct triggering of the SI Thyristor and quenching on the Static Induction Photo-Transistor<sup>11,12)</sup> which is connected to the gate terminal of the SI Thyristor.

The purpose of this paper is to describe the optical direct/indirect triggering and optical quenching mechanisms of the totally light controlled SIP Thy in detail, comparing to the conventional Light Activated Thyristor and GTO. The first experimental results of optically indirect-triggered and quenched GTO will be also described.

### §2. Operational Principle

Fig.1 shows the schematic device cross section of the single-buried-gate SIP Thy with a quenching p-channel SIPT. The optical power directly irradiated on the surface of the SIP Thy can penetrate into the high resistivity n<sup>-</sup> layer around the p<sup>+</sup> gate region being refracted through the beveled surface between gate and cathode electrodes, so that electron-hole pairs are generated in the depletion layer.

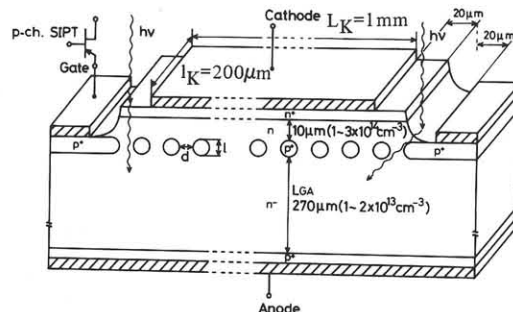


Fig.1 Schematic device structure of the single-buried-gate SIP Thy with a quenching p-channel SIPT, where  $l_K = 200\mu\text{m}$  and  $L_K = 1\text{mm}$ .

Fig.2 shows the energy potential diagram of the single-buried-gate SIP Thy in the forward blocking state. According to the electric field, photogenerated holes are stored at the  $p^+$  gate region, because this region is the energy potential minimum for holes. On the other hand, photo-generated electrons are stored at the  $n^-$  base region near the  $p^+$  anode region. In Fig.2, when the gate potential is positively biased  $\Delta V_G$  resulting from the excessive stored holes  $\Delta P$ , the potential barrier height at the intrinsic gate point  $G^*$  is lowered to  $V_{biG^*K} - \eta\Delta V_G$  so that the electrons in the cathode region have a very small potential barrier height of  $V_{biG^*K} - \eta\Delta V_G$ , although the stored holes in the  $p^+$  gate region have a large barrier height of  $V_{biGK} - \Delta V_G$ . When the gate terminal of the SIP Thy is open-circuited, the maximum D/C optical gain (current gain) of the SIT hook-gate structure at the cathode side is approximately given by the reference 9, 11), as low as the incident optical power,

$$G_{K \max} = \frac{(n_K/p_G) \{ (D_n/W_G) / (D_p/L_p) \} \exp \{ (q/kT) \cdot (V_{biGK} - V_{biG^*K}) \}}{(1)} \quad (1)$$

where  $n_K$  is the electron concentration of the cathode region.  $p_G$  is the hole concentration of the gate region.  $D_n$  is the diffusion constant of electrons,  $D_p$  is the diffusion constant of holes,  $W_G$  is the effective potential barrier width,  $L_p$  is the diffusion length of holes,  $q$  is the unit charge,  $k$  is the Boltzmann's constant,  $T$  is the absolute temperature,  $V_{biGK}$  is the built-in potential between the gate and cathode and  $V_{biG^*K}$  is the potential barrier height at the intrinsic gate point  $G^*$ . The exponential term in equation (1) has a very large value, so that the current gain of the SIP Thy at the cathode side is much larger than those values of the conventional Light Activated Thyristor.

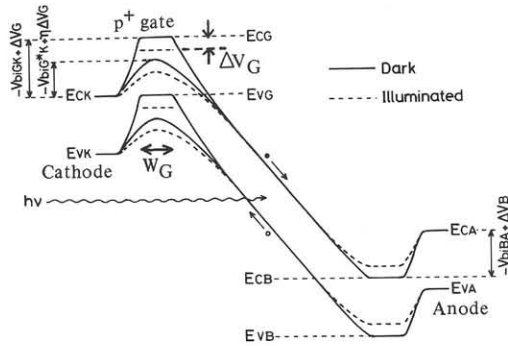


Fig.2 Energy potential diagram of the single-gate SIP Thy and an equivalent circuit at the cathode side.

The turn-off current gain of the SI Thyristor is said to be more than  $10^5$ , so that optically fired SIP Thy can be quenched by the very low power LED light pulse irradiated on the quenching SIPT. Fig. 3(a) and (b) show the experimental circuit diagrams for the direct triggering and quenching, and the indirect triggering and quenching measurement, respectively. In Fig. 3(a), the triggering light pulse (LT) is irradiated on the SIP Thy and the quenching light pulse (LQ) is incident on the quenching p-channel SIPT (TQ). In Fig. 3(b), the triggering LED pulse (LT) is incident on the triggering p-channel SIPT (TT) and the quench LED pulse (LQ) is irradiated on the quenching p-channel SIPT (TQ). Schematic operational waveforms of the triggering LED pulse (LT), the quenching LED pulse (LQ), the anode voltage  $V_{AK}$ , and the anode current  $I_{AK}$  are shown in Fig. 3(c). Response times, such as a turn-on delay time  $T_{don}$ , a rise time  $T_r$ , a turn-off delay time  $T_{doff}$ ,

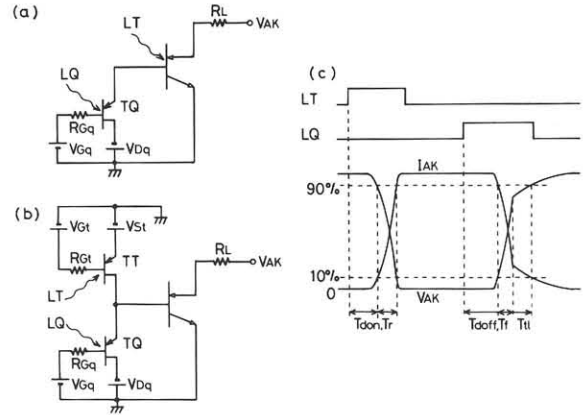


Fig.3 Experimental circuit diagrams: (a) direct trigger and quench, (b) indirect trigger and quench, and (c) operational waveforms.

a fall time  $T_f$ , and a tailing time  $T_{tl}$  are defined in the same figure. In Fig.3(a) and (b), the quenching SIPT (TQ) and the reverse biasing voltage  $V_{Dq}$  are connected seriesely in the gate circuit of the SIP Thy, so that optical triggering and quenching operation of those circuits can be easily understood by the graphical determination of operational points as shown in Fig.4, where the current-voltage characteristics of the gate to cathode pin photodiode and the current-voltage characteristics of the quenching p-channel SIPT as a nonlinear load resistance are illustrated schematically. Operational points A, C, and D correspond to a turn-on state, a turn-off state, and a blocking state, respectively.

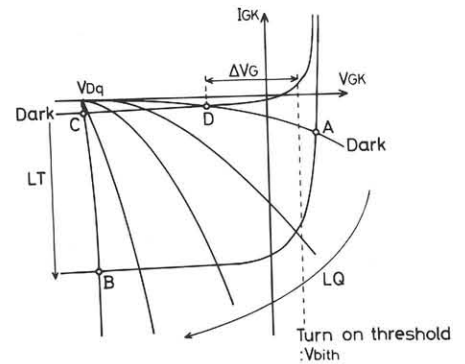


Fig.4 Graphical determination of operational points in the gate circuit.

### §3. Results and Discussion

Measurements are made on the sample having four cathode electrode fingers, one finger area of which is shown in Fig.1. The unit channel length is  $200\mu m$ . The total channel number is 28channels  $\times$  4fingers. Both triggering and quenching LEDs are driven by CMOS logic IC, emitting infrared light ( $\lambda = 880nm$ ) pulses with a rise time of 12nsec.

#### A. Direct triggering and quenching

The turn-on delay time  $T_{don}$  of the normally-off type SIP Thy is plotted as a function of directly triggering LED pulse width  $W_{LT}(nsec)$  for several incident optical powers of  $P_{LT}$  in the Fig.5. When the incident power is increased to be more than  $23\mu W$ , the turn-on delay time  $T_{don}$  decreases below  $1\mu sec$ , and turn-on rise time  $T_r$  is only 380nsec for

this experiment. The turn-on delay time  $T_{don}$  will be determined by the time interval during which the gate potential of the SIP Thy is charged up to the turn-on threshold value of  $V_{bith}$  as shown in Fig.4.

Fig.6 shows the optical switching wave forms of the normally-on type SIP Thy. The anode voltage  $V_{AK}$  of 300V at the anode current  $I_{AK}$  of 2A is directly switched by two LED light pulses having a power of  $P_{LT} = 46.3 \mu W$  and  $P_{LQ} = 60.4 \mu W$ . Turn-on time is  $6.2 \mu sec$  and turn-off time is  $1.5 \mu sec$  for this experiment.

#### B. Indirect triggering and quenching

To speed up the turn-on switching and to reduce the minimum trigger power of the singel-gate SIP Thy much more, one can adopt auxiliary means, such as an amplifying gate structure or an indirectly triggered transistor/thyristor structure. Fig.7 shows the optically indirect-triggered and quenched switching wave forms of the normally-off type SIP Thy. The experimental circuit is shown in Fig.3(b). The anode voltage  $V_{AK}$  of 540V at the anode current  $I_{AK}$  of 1A is indirectly switched with a indirect trigger power of  $P_{LT} = 123 \mu W$  and a quench power of  $P_{LQ} = 1.15 mW$ . Response times are such that,  $T_{don} = 320 nsec$ ,  $T_r = 225 nsec$ ,  $T_{doff} = 1.15 \mu sec$ ,  $T_f = 1.3 \mu sec$  and  $T_{tl} = 4.7 \mu sec$ . The turn-on delay time  $T_{don}$  and the rise time  $T_r$  are plotted as a function of the incident optical power  $P_{LT}$  on the triggering SIPT(TT) for several anode voltages of  $V_{AK}$  in Fig.8. For each  $V_{AK}$ , the turn-off delay time  $T_{doff}$ , the fall time  $T_f$  and the tailing time  $T_{tl}$  are also tabulated in Fig.8. The incident power  $P_{LQ}$  on the quenching p-channel SIPT is  $1.0 mW$  for this experiment. The turn-on delay time  $T_{don}$  is nearly inversely proportional to the increase of the incident power  $P_{LT}$ , though the rise time  $T_r$  is almost independent of the incident power  $P_{LT}$  and is rather much dependent on the value of  $V_{AK}$ .

Response times versus the anode current  $I_{AK}$  characteristics are shown in Fig.9 at the anode voltage  $V_{AK}$  of 540V. The incident power  $P_{LT}$  on the triggering p-channel SIPT is  $123 \mu W$  and the incident power  $P_{LQ}$  on the quenching p-channel SIPT is  $1.15 mW$  for this experiment.

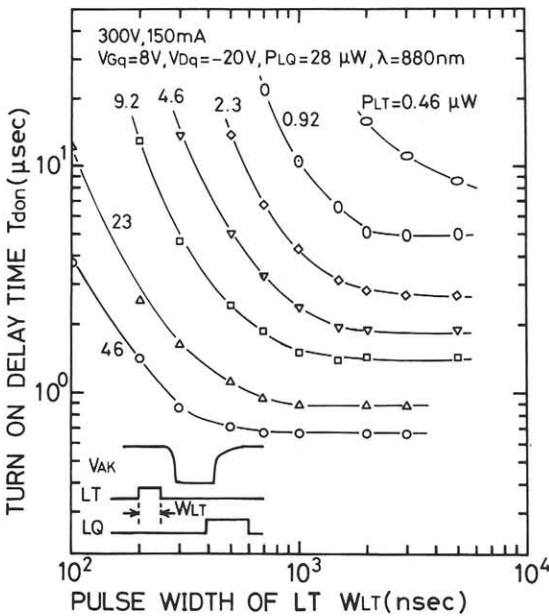


Fig.5 Turn-on delay time  $T_{don}$  versus triggering LED pulse width  $W_{LT}$  for several triggering LED power  $P_{LT}$ .

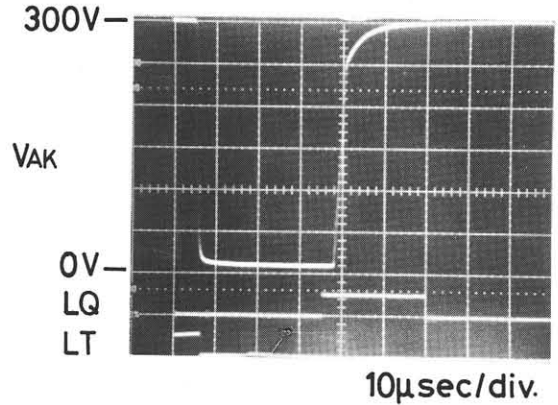


Fig.6 Experimental waveforms of anode voltage  $V_{AK}$ , and direct triggering and quenching LED light pulses (LT, LQ),  $V_{Gq} = 10V$ ,  $R_{Gq} = 100K\Omega$ ,  $V_{Dq} = -35V$  and  $5K\Omega$  of biasing resistance is connected between source and drain of the quenching p-channel SIPT (TQ).

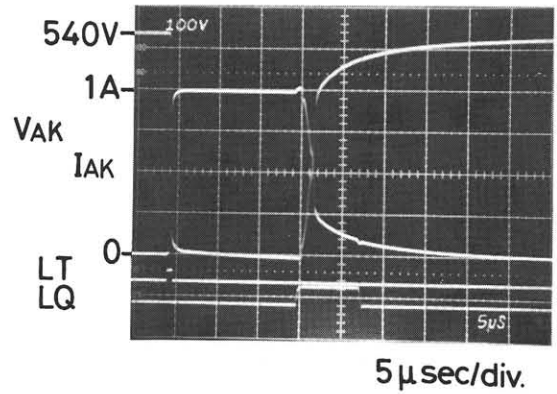


Fig.7 Experimental waveforms of anode voltage  $V_{AK}$ , anode current  $I_{AK}$ , and indirect triggering and quenching LED light pulses (LT, LQ),  $V_{Gq} = 8.3V$ ,  $R_{Gq} = 1M\Omega$ ,  $V_{Dq} = -26V$ ,  $V_{Gt} = 7.5V$ ,  $R_{Gt} = 100K\Omega$ , and  $V_{st} = 5V$ .

#### C. Totally light controlled GTO

Fig.10 shows experimental switching wave forms of the indirectly-triggered and quenched conventional GTO using the same operational circuit shown in Fig.3(b). 400V-10A is indirectly-triggered and quenched in a turn-on time of  $3 \mu sec$  and a turn-off time of  $6 \mu sec$ . The incident LED pulse power  $P_{LT}$  on the triggering p-channel SIPT is  $123 \mu W$  and the incident light power  $P_{LQ}$  on the quenching p-channel SIPT is  $770 \mu W$  for this experiment. However, the same GTO cannot be directly triggered with the same incident trigger power levels of  $12.2 mW/cm^2$ . At this time, the gate potential of GTO is charged up to the value of only  $0.6 eV$ . Moreover, we find the fact that, if we fail to turn-off even a time, the GTO is easy to break.

#### §4. Conclusion

The light trigger sensitivity of the SIP Thy is much higher than that of the conventional Light Activated Thyristor and the GTO, because the optical gain of the SIT gate structure is much larger than that of the bipolar base structure<sup>10,11</sup>. The turn-on threshold voltage of the SIP Thy even for the normally-off type device is smaller than the value of the conventional Light Activated Thyristor. The value of  $dv/dt$  durability of the SIP Thy will be higher

than that of the conventional Light Activated Thyristor, because the reverse gate to cathode voltage at the blocking state (point D, shown in Fig.4) can absorb the displacement current component into the gate circuit. Therefore, SI Thyristor is promising even as a light triggered thyristor. Moreover, totally light controlled SIP Thy has many excellent features of the high speed optical triggering and quenching with the low power LED light, the perfect isolation between power and control circuits, minimizing the number of electrical components simplifying the control circuits, and low-loss in the total systems as compared to the conventional Light Activated Thyristor. And also, as pointed out in the electrical switching<sup>5)</sup>, totally light controlled SIP Thy has the strong feature of being difficult to cause thermal breakdown as compared to the totally light controlled GTO shown in Fig.10.

# References

- 1) J. Nishizawa, T. Terasaki and J. Shibata, "Field Effect Transistor versus Analog Transistor (Static Induction Transistor)", presented at IEDM 1972; presented at ESSDERC 1973; Technical Report of Res. Inst. of Elect. Comm., at Tohoku Univ., RIEC TR-36, 1973; IEEE Trans. on Electron Devices, Vol. ED-22, No.4, 185-197(1975).
- 2) J. Nishizawa and Y. Ohtsubo, "Effects of Gate Structure on Static Induction Thyristor", Tech. Digest of IEDM, Washington, 1980, p. 658.
- 3) Y. Kajiwar, Y. Watakabe, M. Bessho, Y. Yukimoto and K. Shirahata, "A High Speed and High Voltage Static Induction Thyristor", Tech. Digest of IEDM, Washington, 1977, p. 38.
- 4) Y. Terasawa, K. Miyata, S. Murakami, T. Nagano and M. Okamura, "High Power Static Induction Thyristor", Tech. Digest of IEDM, Washington, 1979, p. 250.
- 5) J. Nishizawa, K. Muraoka, Y. Kawamura and T. Tamamushi, "Low Loss High Speed Switching Devices, 2300V-150A Static Induction Thyristor", to be published in IEEE Trans. on Electron Devices, in 1984.
- 6) J. Nishizawa, K. Nakamura, and H. Oka, Japanese Patent Application, No. 51-95585.
- 7) J. Nishizawa, Japanese Patent Application, No.54 - 36079.
- 8) P. Roggwiler, R. Sittig and F. Bernasconi, "Totally Light Controlled Switch and New Means for Electrical Turn-Off of Thyristor", Tech. Digest of IEDM, Washington, 1980, pp. 646-648.
- 9) J. Nishizawa, K. Nonaka and T. Tamamushi, "Static Induction Thyristor", Semiconductor Technologies 1984, JARECT, Vol. 13, edited by J. Nishizawa, (OHM & North-Holland).
- 10) T. Tamamushi, K. Nonaka and J. Nishizawa, "SI Thyristor (in Japanese)", National Convention Record of IEE Japan, S. 7-2-3, 30th March, 1984.
- 11) J. Nishizawa, T. Tamamushi and K. Nonaka, "Current Amplification in non-homogeneous base structure and Static Induction Transistor structure", to be published in Journal of Applied Physics, in 1984.
- 12) J. Nishizawa, T. Tamamushi and S. Suzuki, "SIT Image Converter", Semiconductor Technologies 1983, JARECT, Vol.8, edited by J. Nishizawa (OHM & North-Holland).

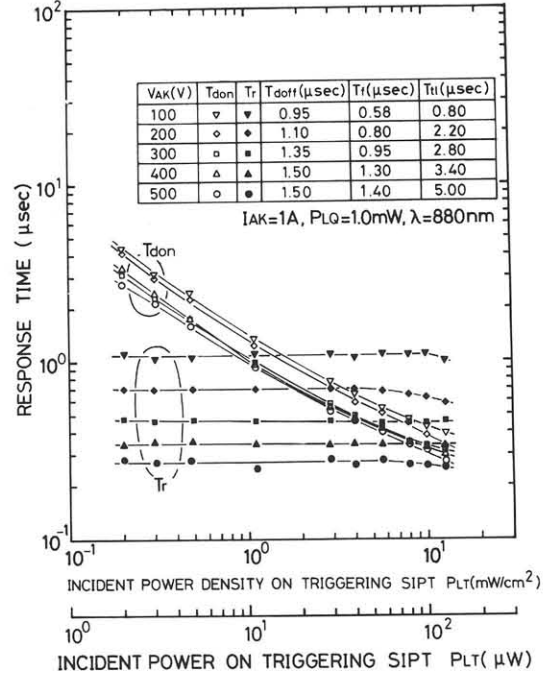


Fig.8 Turn-on delay time  $T_{don}$  and turn-on rise time  $T_r$  versus incident power and power density on triggering SIPT(TT),  $V_{Gq} = 8.5V$ ,  $R_{Gq} = 1M\Omega$ ,  $V_{Dq} = -27V$ ,  $V_{Gt} = 8V$ ,  $R_{Gt} 100K\Omega$ , and  $V_{st} = 5V$ .

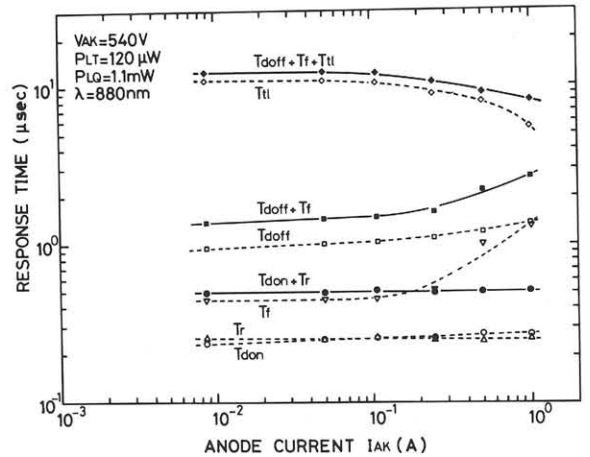


Fig.9 Response times versus anode current  $I_{AK}$  circuit parameters are the same in Fig.8.

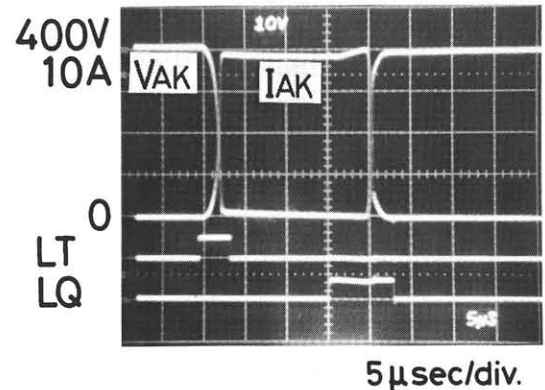


Fig.10 Experimental switching wave forms of indirectly-triggered and quenched conventional GTO,  $V_{Gq} = 4.0V$ ,  $R_{Gq} = 1M\Omega$ ,  $V_{Dq} = -10V$ ,  $V_{Gt} = 10V$ ,  $R_{Gt} = 100K\Omega$ , and  $V_{st} = 4.5V$ .